scientific reports

Check for updates

OPEN

Interfering with USP50 expression inhibits macrophage pyroptosis in sepsis-induced acute lung injury by degrading NLRP3 protein

Shanshan Hu[1], Jingjing Hu[2], Shengnan Shu[1], Yuexuan Chen[3] & Lu Wang[3]✉

Sepsis is a major cause of acute lung injury (ALI) characterized by inflammatory responses. Ubiquitination plays a critical role in the pathogenesis of ALI. This study aimed to investigate the role of USP50, a deubiquitinating enzyme, in sepsis-induced ALI and its underlying molecular mechanisms. THP-1 cells were differentiated into macrophages and exposed to lipopolysaccharide (LPS) to establish an in vitro injury model. Pyroptosis was assessed using immunoblotting, flow cytometry, and enzyme-linked immunosorbent assay. The regulation of USP50 on NLRP3 deubiquitination was analyzed through immunoprecipitation, immunoblotting, and protein stability assays. The in vivo function of USP50 was evaluated using a cecal ligation and puncture (CLP)-induced septic mouse model. Results demonstrated that USP50 expression was significantly upregulated in the blood of patients with sepsis-induced ARDS and in the lungs of CLP-treated mice. USP50 knockdown suppressed pyroptosis in LPS-stimulated macrophages and septic mice. Furthermore, USP50 inhibition enhanced NLRP3 degradation by facilitating K48-linked ubiquitination. Overexpression of NLRP3 reversed the anti-pyroptotic effects induced by USP50 depletion in macrophages. In conclusion, USP50 suppression attenuates macrophage pyroptosis through inhibition of NLRP3 deubiquitination, thereby reducing lung injury in sepsis-induced models. These findings identify USP50 as a potential therapeutic target for sepsis-associated acute lung injury.

Keywords Sepsis-induced acute lung injury, USP50, Deubiquitination, Pyropsosis, NLRP3

Sepsis is a serious systemic inflammatory response syndrome caused by dysregulated host responses to infection[1]. It remains a leading cause of mortality among hospitalized patients, with a reported mortality rate of approximately 30% in China[2,3]. The high mortality is closely associated with multiple organ failure induced by sepsis, including damage to the brain, lungs, and kidneys. Among these organs, the lungs are particularly vulnerable to septic injury. Sepsis-induced acute lung injury (ALI) is characterized by more severe organ dysfunction and higher mortality compared to non-sepsis-induced ALI[4]. Current treatment strategies for sepsis include antibiotics, fluid resuscitation, and organ support therapies[5,6]; however, effective interventions specifically targeting sepsis-induced ALI remain limited. Therefore, further investigation into the pathogenesis of sepsis-induced ALI is critical for developing novel therapeutic strategies and molecular targets.

Sepsis is generally divided into two distinct phases: an initial hyperinflammatory phase following infection and a subsequent immunosuppressive phase after pathogen clearance[7]. During the acute phase, the host mounts a pro-inflammatory response, while in the chronic phase, immune activity shifts toward anti-inflammatory states. This transition often results in severe immune cell dysfunction and mortality[8]. Pyroptosis, a form of inflammatory cell death, is strongly linked to septic pathophysiology. Studies have shown that moderate pyroptosis aids in combating infections, whereas excessive pyroptosis disrupts immune homeostasis[9,10]. As key innate immune cells, macrophages play pivotal roles in these processes. Macrophage pyroptosis has been implicated in sepsis progression and sepsis-induced ALI[11,12]. However, the molecular mechanisms underlying macrophage pyroptosis in sepsis-induced ALI remain poorly understood.

Epigenetic modifications are increasingly recognized as critical regulators of sepsis-related immune responses[13]. Ubiquitination, a post-translational modification, plays essential roles in both physiological

[1]Department of Neurology, Longyou County People's Hospital, Quzhou, Zhejiang, China. [2]Department of Respiratory Medicine, Hangzhou TCM Hospital Affiliated to Zhejiang Chinese Medical University, Hangzhou, Zhejiang, China. [3]Department of Emergency Medicine, Hangzhou TCM Hospital Affiliated to Zhejiang Chinese Medical University, No.453, Stadium Road, Hangzhou 310007, Zhejiang, China. ✉email: 758639564@qq.com

and pathological processes. Dysregulation of the ubiquitin system contributes to the development of diverse diseases, including cancer, metabolic disorders, inflammatory conditions, infections, and neurodegenerative diseases[14]. Ubiquitination governs protein fate by targeting ubiquitin-conjugated proteins for proteasomal degradation, thereby modulating protein activity, localization, and stability[15]. his modification is reversible, with deubiquitinating enzymes (DUBs) removing ubiquitin chains from substrates to maintain free ubiquitin pools under cellular stress conditions[16]. Ubiquitin-specific proteases (USPs), the largest DUB family, are deeply involved in disease-related biological processes[17]. A prior study demonstrated that mitochondrial STAT3 inhibits USP50-mediated deubiquitination of CPT1A, and suppression of mitochondrial STAT3 alleviates LPS-induced sepsis[18], suggesting a potential role for USP50 in septic pathology. However, the specific contribution of USP50 to sepsis-associated lung injury remains largely unexplored.

In this study, we investigated the role of USP50 in regulating macrophage pyroptosis through NLRP3 ubiquitination in vitro and its impact on lung injury in vivo. Our hypothesis posits that USP50 modulates macrophage pyroptosis by deubiquitinating NLRP3, thereby influencing lung damage during sepsis. These findings may provide novel insights into the pathogenesis of sepsis-induced ALI and identify USP50 as a potential therapeutic target for septic lung injury.

Materials and methods

Ethical statement

This study was approved by the Ethics Committee of Hangzhou TCM Hospital Affiliated to Zhejiang Chinese Medical University. Written informed consent was provided by each participant. This study was performed according to the principles of the Declaration of Helsinki.

Clinical samples

Patients with sepsis-induced acute respiratory distress syndrome (ARDS) ($n = 48$) admitted to the intensive care unit (ICU) at our hospital were enrolled in this study. Sepsis was diagnosed according to the Third International Consensus Definitions for Sepsis and Septic Shock (Sepsis-3)[19], while ARDS was diagnosed using the Berlin definition[20]. Whole blood samples were collected from these patients within one hour of ICU admission. Healthy participants ($n = 35$) hospitalized during the same period were also enrolled as controls, and their blood samples were collected under similar conditions.

Cell culture and transfection

Human monocytic THP-1 cells were obtained from Procell (Wuhan, China). The cells were maintained in Roswell Park Memorial Institute (RPMI)-1640 medium (ATCC, Manassas, VA, USA) supplemented with 10% fetal bovine serum (FBS; ATCC) and 1% penicillin/streptomycin (ATCC). Cultures were maintained in a 37 °C incubator with 95% air/5% CO_2. For differentiation, cells were treated with 100 nM phorbol 12-myristate 13-acetate (PMA; Sigma-Aldrich, St. Louis, MO, USA) for 3 days. Following differentiation, macrophages were stimulated with 10 μg/mL lipopolysaccharide (LPS; Sigma-Aldrich) for 8 h.

Small interfering RNA targeting USP50 (si-USP50), non-targeting control siRNA (si-NC), NLRP3 overexpression plasmids (oe-NLRP3), and an empty vector control (oe-NC) were designed and synthesized by GenePharma (Shanghai, China). For transfection, macrophages were seeded into six-well plates and cultured until reaching 70% confluence. Transfection was performed using Lipofectamine 2000 (Invitrogen, Carlsbad, CA, USA) according to the manufacturer's instructions. Cells were harvested 48 h post-transfection for downstream analyses.

Enzyme-linked immunosorbent assay (ELISA)

The levels of interleukin (IL)-1β and IL-18 in mouse serum and macrophage culture supernatant were quantified using mouse/human IL-1β and IL-18 ELISA kits (Elabscience, Wuhan, China), respectively, according to the manufacturer's instructions.

Flow cytometry

Pyroptosis was assessed using the FLICA 660 caspase-1 assay kit (ImmunoChemistry Technologies, Bloomington, MN, USA) following the manufacturer's instructions. In brief, FLICA reagent was diluted in PBS at a 1:5 ratio. Macrophages (approximately 1×10^5 cells) were incubated with 10 μL of diluted FLICA reagent for 1 h. After three washes with 1× cell wash buffer, the cells were incubated with 50 μg/mL propidium iodide for 10 min in the dark. Pyroptosis was analyzed using a flow cytometer.

Quantitative real-time polymerase chain reaction (qPCR)

Total RNA was extracted from participant whole blood, macrophages, and lung tissues using TRIzol reagent (Invitrogen). RNA concentration and purity were measured using the NanoDrop™ One/OneC microvolume spectrophotometer (ThermoFisher Scientific, Waltham, MA, USA). Subsequently, total RNA was reverse-transcribed into first-strand cDNA using the PrimeScript™ FAST RT reagent kit with gDNA eraser (Takara, Tokyo, Japan). Quantitative real-time PCR (qPCR) was performed using the TB Green Premix Ex Taq™ II (Tli RNaseH Plus) (Takara) on the Applied Biosystems 7500 real-time PCR system (ThermoFisher Scientific). RNA expression levels were analyzed using the $2^{-\Delta\Delta Ct}$ method, with GAPDH serving as the internal control.

Immunoblotting

Proteins were extracted from macrophages and lung tissues using radioimmunoprecipitation assay lysis buffer. Protein concentrations were quantified using a bicinchoninic acid (BCA) protein colorimetric assay kit (Elabscience). A total of 30 μg of protein per sample was loaded into each lane of a 10% sodium dodecyl sulfate

(SDS)-polyacrylamide gel for electrophoretic separation, followed by transfer onto polyvinylidene fluoride membranes. Membranes were incubated with primary antibodies at 4 °C overnight and subsequently incubated with secondary antibodies for 1 h at room temperature. Protein bands were visualized using an enhanced chemiluminescent substrate detection kit (Elabscience).

Protein stability assay
Following USP50 knockdown, macrophages were treated with 100 μM cycloheximide (CHX; Sigma-Aldrich) for 0, 3, 6, and 12 h. NLRP3 protein levels were analyzed via immunoblotting.

Immunoprecipitation (IP)
Macrophages were lysed in IP buffer, and the supernatant was collected after centrifugation at 12,000 × g for 10 min. Subsequently, the lysate was incubated with specific antibodies and isotype control IgG (e.g., mouse IgG) for 2 h at 4 °C. Protein A/G magnetic beads were then added and incubated at 4 °C for 1 h. The mixture was washed three times with IP buffer to remove nonspecifically bound proteins. The beads were eluted with an appropriate elution buffer, and the immunoprecipitated proteins were analyzed via immunoblotting to detect target protein levels.

Animal study
C57BL/6 mice (male, 6–8 weeks old, body weight 22–25 g) were obtained from Slkjd (Changsha, China). The mice were randomly assigned to four groups: sham, cecal ligation puncture (CLP), CLP + short hairpin RNA lentivirus (LV-shNC), and CLP + short hairpin RNA targeting USP50 lentivirus (LV-shUSP50), with six mice per group. To establish the sepsis model, CLP surgery was performed[21]. Briefly, mice were anesthetized via inhalation of 3% isoflurane (Sigma-Aldrich) and maintained with 1.5% isoflurane. A 1 cm longitudinal midline incision was made in the lower abdomen. The distal ileocecal valve was ligated and the cecum was punctured using a 20-gauge needle. A portion of cecal contents was collected and reintroduced into the abdominal cavity before suture closure of both the cecum and abdominal wall. Normal saline (1 mL) was administered subcutaneously for fluid resuscitation. Sham-operated mice underwent identical surgical procedures without cecal ligation, puncture, or fecal inoculation. Two days prior to CLP surgery, mice in the CLP + LV-shNC and CLP + LV-shUSP50 groups received tail vein injections of lentivirus (4×10^8 TU per mouse). All animals were euthanized 24 h post-surgery via inhalation of 5% isoflurane. Whole blood and lung tissues were collected, with serum obtained after centrifugation at 1000 × g for 20 min. This study was approved by the Ethics Committee of Hangzhou TCM Hospital Affiliated to Zhejiang Chinese Medical University. All animal experiments were conducted in accordance with the ARRIVE guidelines and relevant institutional regulations.

Determination of wet/dry ratio
The right upper lobe was rinsed with normal saline and weighed. After drying at 60 °C for 3 days, the sample was reweighed. The wet/dry weight ratio was calculated.

Hematoxylin and eosin (H&E) staining assay
The lungs were fixed in 10% formalin for 24 h and paraffin-embedded. Subsequently, 5-μm-thick paraffin sections were cut. After deparaffinization and rehydration, the sections were stained with the HE staining kit (Solarbio, Beijing, China) according to the manufacturer's instructions. The stained sections were visualized under a light microscope.

Statistical analysis
Statistical analysis was performed using GraphPad Prism 8 software. Results are presented as mean ± SD. Comparisons were conducted using Student's t-test, one-way ANOVA, and two-way ANOVA. Independent determinants associated with sepsis-induced ARDS were analyzed using multivariate logistic regression. The overall survival of patients with sepsis-induced ARDS stratified by high/low USP50 expression was evaluated using Kaplan-Meier survival analysis. The diagnostic utility of USP50 was assessed via Receiver Operating Characteristic (ROC) curve analysis, with diagnostic accuracy quantified by the Area Under the Curve (AUC). A P value < 0.05 was considered statistically significant.

Results
USP50 is highly expressed in patients with sepsis-induced ARDS and CLP-induced mice
To investigate the role of USP50 in sepsis-induced ALI, we enrolled 48 patients with sepsis-induced ARDS and 35 healthy controls. Baseline clinical characteristics of all participants are summarized in Table 1. The normal control group included 16 males with a mean age of 43.4 years, while the sepsis-induced ARDS group comprised 24 males with a mean age of 43.2 years. Regarding pre-existing comorbidities, no significant differences were observed in chronic obstructive pulmonary disease (COPD), liver disease, diabetes, or obesity between the two groups. However, coronary artery disease (CAD), hypertension, and chronic kidney disease (CKD) showed marked differences between healthy controls and patients with sepsis-induced ARDS. In terms of pathogens, no significant differences were found in Gram-positive bacteria, Gram-negative bacteria, viral infections, other pathogens, or undetected pathogens. However, fungal infections were significantly different between the groups. USP50 expression was initially measured using qPCR. In the blood of patients with sepsis-induced ARDS, USP50 expression was significantly elevated compared to healthy controls (Fig. 1A). Subsequently, patients with sepsis-induced ARDS were stratified into survivors and non-survivors based on 28-day hospitalization outcomes. Significant differences were observed in hypertension, diabetes, Gram-negative bacterial infections, and USP50 expression between the survivor and non-survivor groups (Table 2). Multivariable logistic regression

	Normal ($N=35$)	Sepsis-induced ARDS ($N=48$)	p
Gender(male,%)	16(45.7%)	24(50%)	0.991
Ages (years), mean ± SD	43.4 ± 11.9	43.2 ± 11.6	0.929
Pre-existing comorbidities			
COPD, n(%)	8(22.86%)	4(8.33%)	0.065
CAD, n(%)	9(25.71%)	3(6.25%)	0.013
Hypertension, n(%)	3(8.57%)	23(47.92%)	< 0.001
CKD, n(%)	10(28.57%)	3(6.25%)	0.006
Liver disease, n(%)	2(5.71%)	4(8.33%)	0.651
Diabetes, n(%)	1(2.86%)	6(12.50%)	0.121
Obesity, n(%)	2(5.71%)	5(10.42%)	0.449
Pathogen			
Gram-positive bacteria, n(%)	4(11.43%)	9(18.75%)	0.368
Gram-negative bacteria, n(%)	2(5.71%)	9(18.75%)	0.086
Virus, n(%)	5(14.29%)	10(20.83%)	0.447
Fungus, n(%)	11(31.43%)	5(10.42%)	0.017
Other pathogens, n(%)	9(25.71%)	8(16.67%)	0.316
Undetected, n(%)	4(11.43%)	7(14.58%)	0.677

Table 1. Baseline characteristics of healthy controls and patients with sepsis-induced ARDS. COPD, chronic obstructive pulmonary disease; CAD, coronary artery disease; CKD, chronic kidney disease.

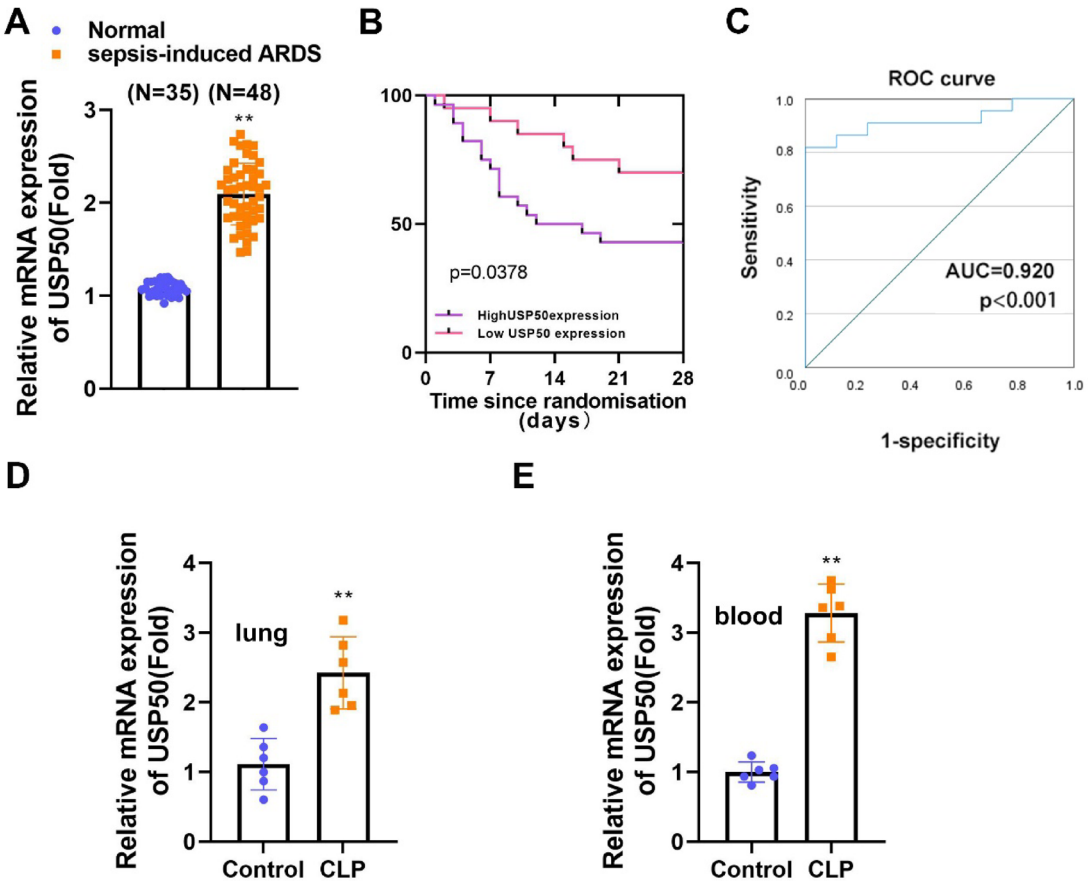

Fig. 1. USP50 is highly expressed in patients with sepsis-induced ARDS and CLP-induced mice. (**A**) USP50 expression was measured in patients with sepsis-induced ARDS ($n=48$) and healthy controls ($n=35$) using qPCR. (**B**) Patients with sepsis-induced ARDS were divided into USP50 high (fold ≥ 2; $n=28$) and low (fold < 2; $n=20$) expression groups, and the overall survival was calculated. (**C**) The diagnostic value of USP50 was analysed using the ROC curve. (**D**) USP50 expression was measured using qPCR in the lung tissues of mice in the sham and CLP groups ($n=6$). (**E**) USP50 expression was measured in the blood of mice using qPCR in the sham and CLP groups ($n=6$). $^{**}P<0.01$.

	Survival($N=26$)	Non-survivors ($N=22$)	p
Gender(male,%)	14(53.85%)	10(45.45%)	0.566
Ages (years), mean ± SD	43.85 ± 11.36	42.36 ± 12.11	0.411
Pre-existing comorbidities			
COPD, n(%)	4(15.38%)	0(0%)	0.057
CAD, n(%)	1(3.85%)	2(9.09%)	0.459
Hypertension, n(%)	6(23.08%)	17(77.27%)	< 0.001
CKD, n(%)	3(11.54%)	0(0%)	0.103
Liver disease, n(%)	3(11.54%)	1(4.55%)	0.387
Diabetes, n(%)	6(23.08%)	0(0%)	0.017
Obesity, n(%)	3(11.54%)	2(9.09%)	0.784
Pathogen			
Gram-positive bacteria, n(%)	6(23.08%)	3(13.64%)	0.409
Gram-negative bacteria, n(%)	2(7.69%)	7(31.82%)	0.035
Virus, n(%)	5(19.23%)	5(22.73%)	0.769
Fungus, n(%)	4(15.38%)	1(4.55%)	0.225
Other pathogens, n(%)	6(23.08%)	2(9.09%)	0.200
Undetected, n(%)	3(11.54%)	4(18.18%)	0.520
USP50	1.92 ± 0.25	2.31 ± 0.30	< 0.001

Table 2. Baseline characteristics of survivors and non-survivors (28-day hospital outcomes). COPD, chronic obstructive pulmonary disease; CAD, coronary artery disease; CKD, chronic kidney disease.

variable	B	Wald	p	OR	95% CI
Hypertension	3.023	6.617	0.010	20.550	2.054-205.633
Gram-negative bacteria	1.612	1.092	0.296	5.013	0.244-103.031
USP50	6.855	9.912	0.002	948.216	13.294-67632.119

Table 3. Multivariable logistic regression analysis of risk factors for sepsis-induced ARDS.

analysis identified hypertension and USP50 expression as independent risk factors associated with sepsis-induced ARDS (Table 3). Patients with sepsis-induced ARDS were further divided into high- and low-USP50 expression groups. High USP50 expression was significantly associated with poor overall survival ($p=0.0378$; Fig. 1B). Additionally, the the AUC value was 0.920 ($p<0.001$; Fig. 1C). To validate these findings in vivo, a cecal ligation and puncture (CLP) mouse model of sepsis was established. USP50 expression in murine lungs was evaluated, and qPCR results revealed higher USP50 expression in the lungs and blood of CLP-induced mice compared to the sham group (Fig. 1D and E). These findings suggest that USP50 may play a role in sepsis, particularly in the pathogenesis of lung injury.

Interfering with USP50 inhibits LPS-induced pyroptosis of macrophages

Next, the role of USP50 in macrophage pyroptosis was assessed. THP-1 cells were differentiated into macrophages using PMA. si-USP50 transfection significantly reduced USP50 mRNA and protein levels in macrophages (Fig. 2A). Subsequently, macrophages were stimulated with LPS to model inflammatory activation. Pyroptosis, characterized by active caspase-1, was analyzed via flow cytometry. Results demonstrated that LPS induced pyroptosis, whereas USP50 knockdown inhibited LPS-induced pyroptosis (Fig. 2B,C). Levels of IL-1β and IL-18 were elevated in LPS-treated cells, but this increase was attenuated by USP50 knockdown (Fig. 2D and E). Pyroptosis-associated protein expression was quantified using immunoblotting. LPS treatment upregulated ASC, NLRP3, GSDMD-N, and cleaved caspase-1 levels, downregulated pro-caspase-1, and had no effect on GSDMD expression. However, USP50 knockdown reversed the LPS-induced alterations in these protein levels (Fig. 2F). Collectively, LPS induces macrophage pyroptosis, and suppression of USP50 attenuates pyroptosis in LPS-stimulated macrophages.

USP50 stabilizes NLRP3 by K48-linked deubiquitination

We next examined the regulatory mechanism of USP50 on NLRP3 expression. USP50 knockdown had no effect on NLRP3 mRNA levels (Fig. 3A) but significantly reduced NLRP3 protein abundance (Fig. 3B). Given the deubiquitinating activity of USP50, we investigated whether NLRP3 undergoes ubiquitination modification. Co-immunoprecipitation experiments confirmed that USP50 physically interacts with NLRP3 (Fig. 3C). In the presence of the proteasome inhibitor MG132, NLRP3 ubiquitination levels increased, whereas Myc-USP50 overexpression reversed this effect (Fig. 3D). Additionally, USP50 knockdown enhanced NLRP3 ubiquitination (Fig. 3E). Ubiquitination typically occurs via degradative K48-linked chains or non-degradative K63-linked chains[22]. To determine the specific linkage type, we assessed K48-linked ubiquitination of NLRP3. In the WT

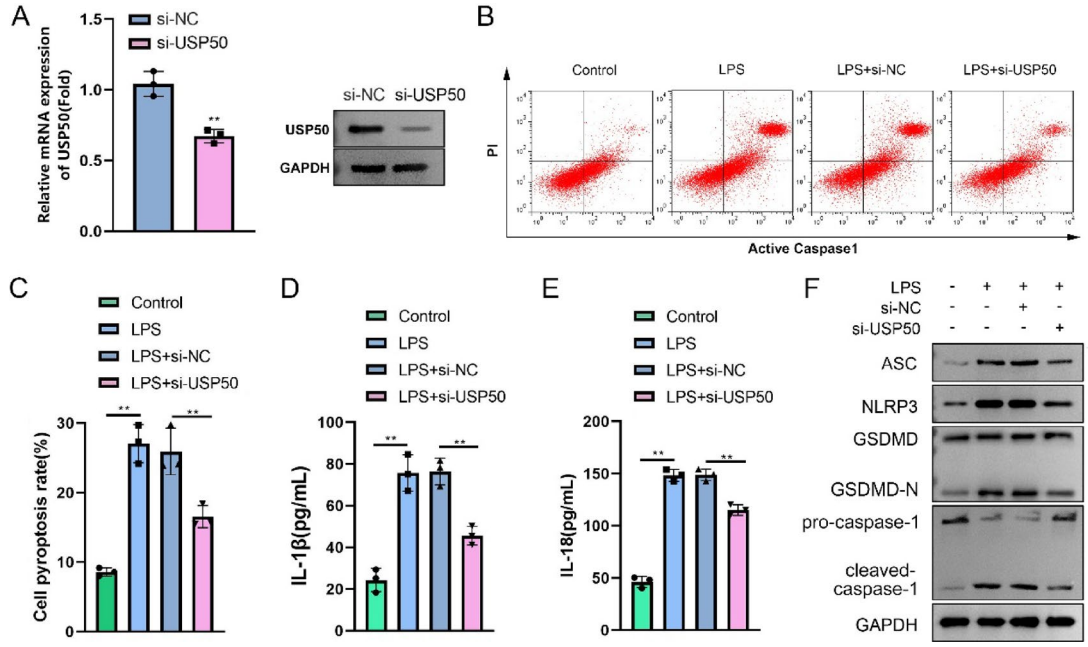

Fig. 2. Interfering with USP50 inhibits LPS-induced pyroptosis of macrophages. (**A**) THP-1 cells were treated with PMA to obtain macrophage phenotype. These macrophages were transfected with si-USP50 and si-NC, and the mRNA and protein levels of USP50 was measured by qPCR and immunoblotting, respectively. (**B**) Flow cytometry was performed to determine cell pyroptosis, and (**C**) pyroptosis rate was quantified. (**D**) IL-1β and (**E**) IL-18 levels in the supernatant of the cell culture medium were detected using ELISA. (**F**) The levels of pyroptosis-related proteins including ASC, NLRP3, GSDMD, GSDMD-N, pro-caspase-1, and cleaved caspase-1 were detected using immunoblotting. ($n = 3$). Original blots are presented in Supplementary Fig. 1. $^{**}P < 0.01$.

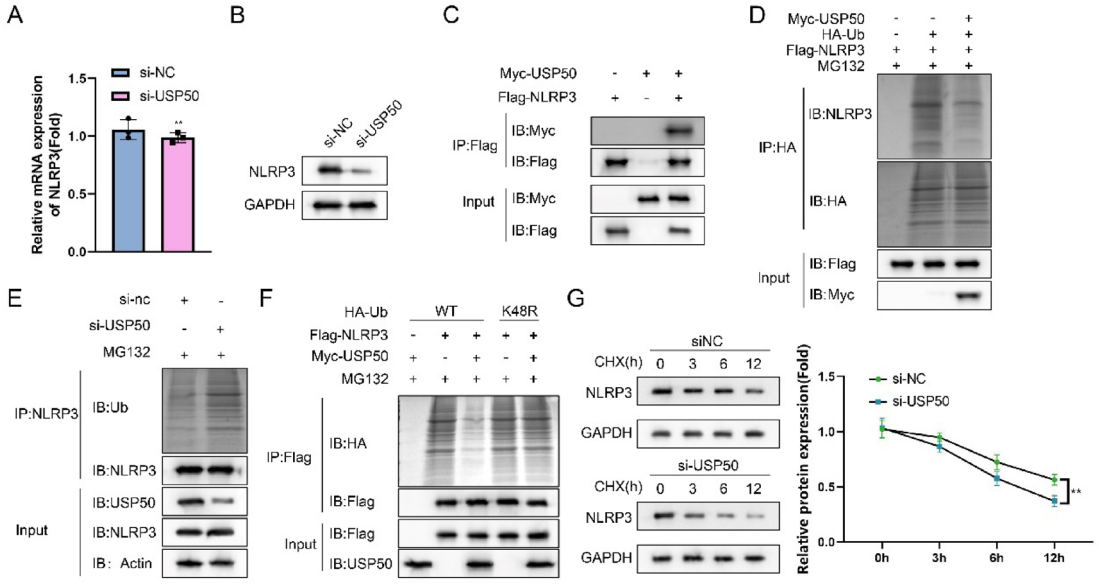

Fig. 3. USP50 stabilizes NLRP3 by K48-linked deubiquitination. (**A**) qPCR and (**B**) immunoblotting were conducted to determine the effect of USP50 on the expression of NLRP3. (**C**) After IP of the Flag, the protein levels of NLRP3 were measured by immunoblotting to assess the interaction between USP50 and NLRP3. (**D**) The effect of USP50 on the ubiquitination levels of NLRP3 in the presence of HA-Ub and MG132. (**E**) After knocking down of USP50, the ubiquitination levels of NLRP3 were measured by IP and immunoblotting. (**F**) When the Ub-K48 chain was mutated, the ubiquitination of NLRP3 influenced by USP50 was measured using immunoblotting. (**G**) The protein stability of NLRP3 was detected using immunoblotting after USP50 silence. ($n = 3$). Original blots are presented in Supplementary Fig. 2. $^{**}P < 0.01$. ns: no significance.

group, USP50 reduced NLRP3 ubiquitination levels. However, co-expression of NLRP3 with the ubiquitin mutant Ub-K48R did not alter ubiquitination levels (Fig. 3F). Furthermore, USP50 knockdown shortened the half-life of NLRP3 protein (Fig. 3G). Collectively, these findings indicate that USP50 promotes K48-linked deubiquitination of NLRP3, thereby stabilizing NLRP3 protein.

Overexpression of NLRP3 abrogated the inhibition of macrophage pyroptosis induced by USP50 knockdown

Rescue experiments were conducted to evaluate the role of the USP50/NLRP3 axis in macrophage pyroptosis. oe-NLRP3 significantly increased NLRP3 mRNA and protein levels in macrophages (Fig. 4A). Subsequently, pyroptosis was assessed. USP50 knockdown suppressed the pyroptosis rate, whereas NLRP3 overexpression counteracted this suppression (Fig. 4B,C). Furthermore, overexpression of NLRP3 reversed the inhibition of IL-1β and IL-18 release in LPS-stimulated cells caused by USP50 knockdown (Fig. 4D and E). Additionally, USP50 knockdown downregulated the levels of ASC, NLRP3, GSDMD-N, and cleaved caspase-1 while upregulating pro-caspase-1 levels. These effects were reversed by NLRP3 overexpression (Fig. 4F). Collectively, suppression of USP50 inhibits macrophage pyroptosis by downregulating NLRP3 expression.

Silencing of USP50 attenuates lung injury in CLP mice via inhibiting pyroptosis

The in vivo role of USP50 was evaluated in a CLP-induced sepsis model. LV-shUSP50 and LV-shNC were administered via tail vein injection prior to CLP surgery. LV-shUSP50 significantly reduced USP50 expression in the lungs of CLP-induced mice (Fig. 5A). Lung injury was assessed using H&E staining. As shown in Fig. 5B, CLP exacerbated lung injury compared to the sham group, whereas USP50 knockdown ameliorated lung damage in CLP-induced septic mice. The lung wet/dry weight ratio, a marker of pulmonary edema, was elevated in CLP mice but attenuated by USP50 knockdown (Fig. 5C). Serum levels of IL-1β and IL-18 were increased in CLP mice, and this increase was reversed by USP50 knockdown (Fig. 5D and E). Furthermore, CLP upregulated the expression of pyroptosis-related proteins, including ASC, NLRP3, GSDMD-N, and cleaved caspase-1, while downregulating pro-caspase-1 levels in lung tissues. However, USP50 knockdown counteracted these CLP-induced alterations (Fig. 5F). Collectively, suppression of USP50 alleviates lung injury in septic mice by inhibiting pyroptosis.

Discussion

The pyroptosis-induced inflammatory response has garnered increasing attention in various diseases due to the release of pro-inflammatory cytokines, including IL-1β and IL-18, through plasma membrane pores

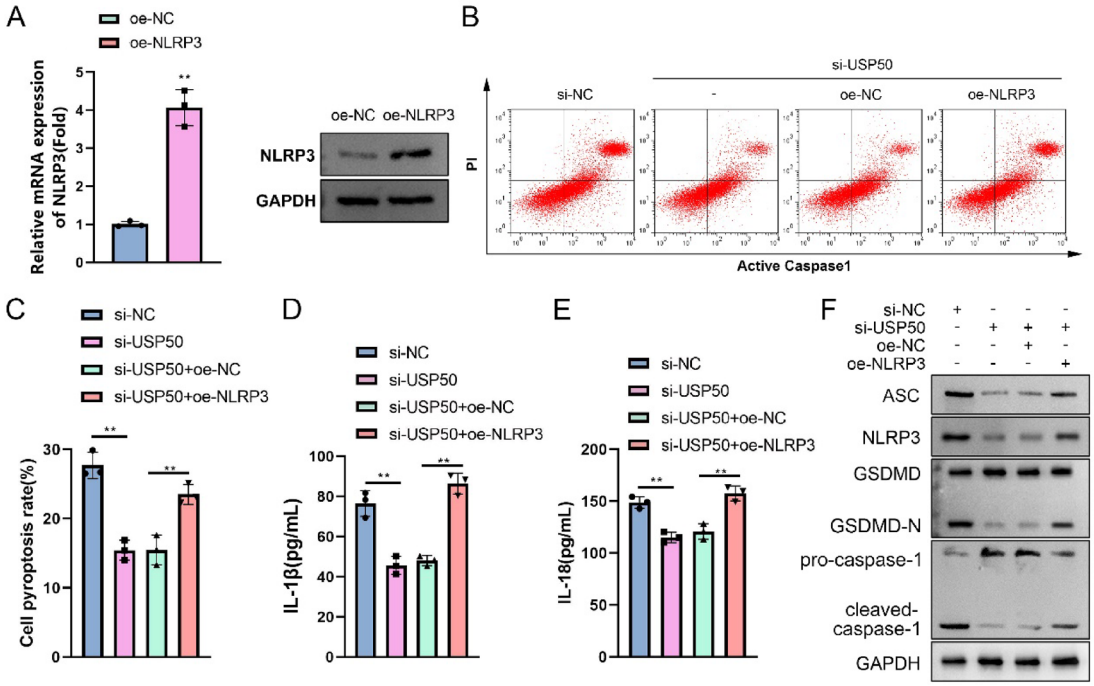

Fig. 4. Overexpression of NLRP3 abrogated the inhibition of macrophage pyroptosis induced by USP50 knockdown. (**A**) The expression of NLRP3 was detected in macrophages using qPCR and immunoblotting after transfection with oe-NC and oe-NLRP3. (**B**) Cell pyroptosis was evaluated by flow cytometry, and (**C**) the pyroptosis rate was quantified. (**D**) IL-1β and (**E**) IL-18 levels in the supernatant of the cell culture medium were detected using ELISA. (**F**) ASC, NLRP3, GSDMD, GSDMD-N, pro-caspase-1, and cleaved caspase-1 protein levels were detected using immunoblotting. ($n = 3$). Original blots are presented in Supplementary Fig. 3. $^{**}P < 0.01$.

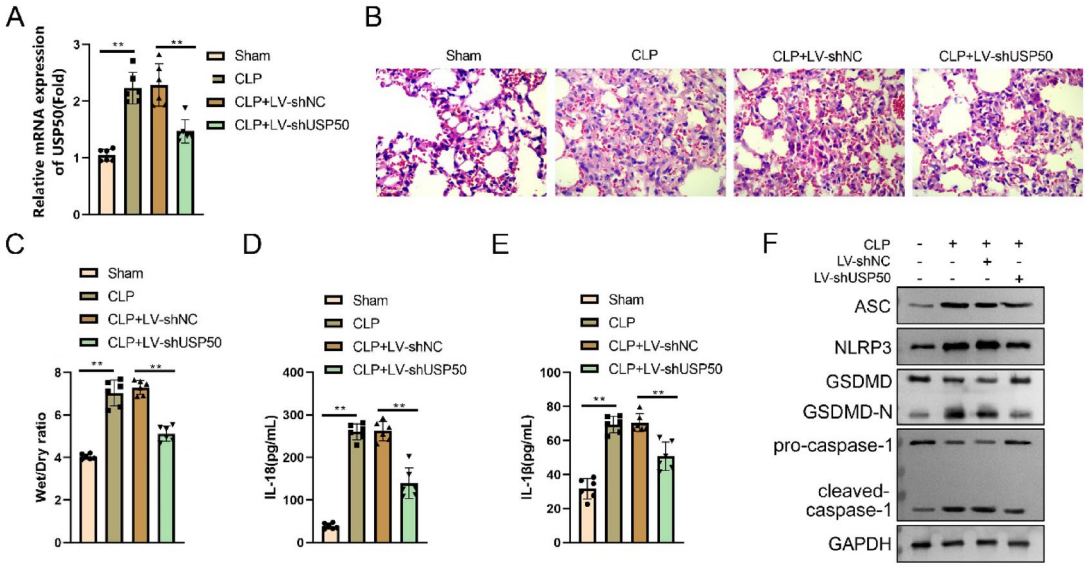

Fig. 5. Silencing of USP50 attenuates lung injury in CLP mice via inhibiting pyroptosis. (**A**) USP50 expression in the lungs of mice in each group was measured by qPCR. (**B**) Lung injury was evaluated using H&E staining assay. (**C**) The wet/dry ratio of lungs was quantified. (**D**) IL-1β and (**E**) IL-18 levels in the serum of mice were measured using ELISA. (**F**) ASC, NLRP3, GSDMD, GSDMD-N, pro-caspase-1 and cleaved caspase-1 protein levels in the lungs of mice were examined using immunoblotting. ($n = 6$). Original blots are presented in Supplementary Fig. 4. $^{**}P < 0.01$.

formed during pyroptosis. In the acute phase of sepsis, macrophages undergo massive pyroptosis to promote the release of these cytokines, which aid in host defense against infections. However, excessive accumulation of pro-inflammatory mediators exacerbates tissue damage and worsens sepsis outcomes[23]. During the immunosuppressive phase of sepsis, macrophages exhibit reduced capacity to produce pro-inflammatory cytokines, suggesting that pyroptosis is suppressed[24]. Recent studies have focused on macrophage pyroptosis in sepsis, particularly in sepsis-induced ALI. For instance, alpha-linolenic acid attenuates macrophage pyroptosis in lung tissues, thereby mitigating sepsis-induced ALI[25]. Similarly, BRD3308 alleviates lung damage in septic models by inhibiting NLRP3-mediated macrophage pyroptosis[26]. Despite these advances in understanding the regulatory mechanisms of pyroptosis in sepsis-induced ALI, comprehensive insights into the molecular pathways remain limited.

USP50 has been implicated in macrophage pyroptosis. Zhao et al.[27] demonstrated that USP50 expression is upregulated in duodenogastric reflux-associated macrophages, which subsequently promotes NLRP3 inflammasome activation and accelerates pyroptotic cell death. Accumulating evidence indicates that USP50 plays critical pathogenic roles in multiple diseases, including SARS-CoV-2 infection, tendinopathy, and sepsis[18,28,29]. In sepsis, previous research has only established that STAT3 drives USP50-mediated CPT1a regulation of fatty acid oxidation. However, whether USP50 modulates macrophage pyroptosis specifically in sepsis-induced ALI remains elusive. In our current investigation, experimental results revealed that USP50 knockdown significantly inhibited pyroptosis in LPS-induced macrophages in vitro and CLP-induced pulmonary pyroptosis in mouse models. Furthermore, genetic suppression of USP50 markedly attenuated lung injury in CLP-induced septic mice. These findings suggest that USP50 inhibition may alleviate sepsis-related lung damage through suppression of macrophage pyroptosis pathways.

Although numerous DUBs have been identified, their functional mechanisms remain largely uncharacterized. Notably, DUBs are well established for their capacity to remove ubiquitin moieties from ubiquitinated substrates. As a DUB, we investigated the role of USP50 in NLRP3 deubiquitination. Our findings demonstrated that USP50 physically interacts with NLRP3, and its knockdown significantly increased NLRP3 ubiquitination levels. Accumulating evidence suggests that ubiquitinated NLRP3 contributes to macrophage pyroptosis. For instance, GITR promotes NLRP3 inflammasome-mediated pyroptosis by reducing ubiquitination and enhancing acetylation of NLRP3[11]. Neutrophil extracellular traps facilitate NLRP3 deubiquitination, activating pyroptotic signaling in alveolar macrophages and exacerbating sepsis-induced acute lung injury[30]. While prior studies indicate that USP50 regulates pyroptosis through ASC deubiquitination[27,31]; however, no studies have investigated the ubiquitination of NLRP3 by USP50. Ubiquitin is assembled into the multiubiquitin chain by seven lysine residues in ubiquitin[32]. NLRP3 has been revealed to be ubiquitinated by K63 and K48 chains[33]. K48-linked ubiquitination is well established to drive proteasomal degradation[34], whereas K63-linked ubiquitination participates in proteasome-independent processes including DNA repair, endocytosis, and signal transduction[35]. In our study, we specifically identified K48-linked ubiquitination and observed that USP50 knockdown enhanced K48-linked ubiquitination of NLRP3, thereby reducing its protein stability. This study identifies a novel regulatory mechanism by which USP50 modulates pyroptosis. These findings suggest that USP50 exerts multifaceted regulatory roles in inflammasome activation through distinct molecular targets, including both

ASC and NLRP3. Furthermore, overexpression of NLRP3 reversed the anti-pyroptotic effects induced by USP50 knockdown. Collectively, these results demonstrate that USP50 silencing inhibits pyroptosis primarily through K48-linked ubiquitination-mediated destabilization of NLRP3.

In conclusion, USP50 functions as a negative regulator of macrophage pyroptosis in sepsis-induced ALI. Mechanistically, genetic suppression of USP50 induces K48-linked ubiquitination of NLRP3, thereby diminishing its protein stability. Our findings reveal a novel molecular mechanism underlying sepsis-induced ALI and identify USP50 as a potential therapeutic target for intervention in this pathological process.

Data availability

The datasets used and/or analysed during the current study are available from the corresponding author on reasonable request.

Received: 17 April 2025; Accepted: 8 July 2025
Published online: 23 July 2025

References

1. Wang, W. & Liu, C. F. Sepsis heterogeneity. *World J. Pediatr.* **19**, 919–927. https://doi.org/10.1007/s12519-023-00689-8 (2023).
2. Font, M. D., Thyagarajan, B. & Khanna, A. K. Sepsis and septic shock—basics of diagnosis, pathophysiology and clinical decision making. *Med. Clin. North. Am.* **104**, 573–585. https://doi.org/10.1016/j.mcna.2020.02.011 (2020).
3. Liu, Y. C. et al. Frequency and mortality of sepsis and septic shock in china: A systematic review and meta-analysis. *BMC Infect. Dis.* **22**, 564. https://doi.org/10.1186/s12879-022-07543-8 (2022).
4. Gao, M. et al. Sepsis plasma-derived exosomal miR-1-3p induces endothelial cell dysfunction by targeting SERP1. *Clin. Sci. (Lond)* **135**, 347–365. https://doi.org/10.1042/CS20200573 (2021).
5. Liu, D. et al. Sepsis-induced immunosuppression: Mechanisms, diagnosis and current treatment options. *Mil Med. Res.* **9**, 56. https://doi.org/10.1186/s40779-022-00422-y (2022).
6. Vincent, J. L. Current sepsis therapeutics. *EBioMedicine* **86**, 104318. https://doi.org/10.1016/j.ebiom.2022.104318 (2022).
7. Nedeva, C. Inflammation and cell death of the innate and adaptive immune system during sepsis. *Biomolecules* **11** https://doi.org/10.3390/biom11071011 (2021).
8. Hotchkiss, R. S., Monneret, G. & Payen, D. Sepsis-induced immunosuppression: From cellular dysfunctions to immunotherapy. *Nat. Rev. Immunol.* **13**, 862–874. https://doi.org/10.1038/nri3552 (2013).
9. Zheng, X., Chen, W., Gong, F., Chen, Y. & Chen, E. The role and mechanism of pyroptosis and potential therapeutic targets in sepsis: A review. *Front. Immunol.* **12**, 711939. https://doi.org/10.3389/fimmu.2021.711939 (2021).
10. Zhu, C., Liang, Y., Luo, Y. & Ma, X. Role of pyroptosis in hemostasis activation in sepsis. *Front. Immunol.* **14**, 1114917. https://doi.org/10.3389/fimmu.2023.1114917 (2023).
11. Liang, S. et al. GITR exacerbates lysophosphatidylcholine-induced macrophage pyroptosis in sepsis via posttranslational regulation of NLRP3. *Cell. Mol. Immunol.* https://doi.org/10.1038/s41423-024-01170-w (2024).
12. Tao, Y., Xu, X., Yang, B., Zhao, H. & Li, Y. Mitigation of Sepsis-Induced acute lung injury by BMSC-Derived Exosomal miR-125b-5p through STAT3-Mediated suppression of macrophage pyroptosis. *Int. J. Nanomed.* **18**, 7095–7113. https://doi.org/10.2147/IJN.S441133 (2023).
13. Wu, D., Shi, Y., Zhang, H. & Miao, C. Epigenetic mechanisms of immune remodeling in sepsis: Targeting histone modification. *Cell. Death Dis.* **14**, 112. https://doi.org/10.1038/s41419-023-05656-9 (2023).
14. Popovic, D., Vucic, D. & Dikic, I. Ubiquitination in disease pathogenesis and treatment. *Nat. Med.* **20**, 1242–1253. https://doi.org/10.1038/nm.3739 (2014).
15. Kitamura, H. Ubiquitin-Specific proteases (USPs) and metabolic disorders. *Int. J. Mol. Sci.* **24** https://doi.org/10.3390/ijms24043219 (2023).
16. Snyder, N. A. & Silva, G. M. Deubiquitinating enzymes (DUBs): Regulation, homeostasis, and oxidative stress response. *J. Biol. Chem.* **297**, 101077. https://doi.org/10.1016/j.jbc.2021.101077 (2021).
17. Chen, S., Liu, Y. & Zhou, H. Advances in the development ubiquitin-specific peptidase (USP) inhibitors. *Int. J. Mol. Sci.* **22** https://doi.org/10.3390/ijms22094546 (2021).
18. Li, R. et al. Mitochondrial STAT3 exacerbates LPS-induced sepsis by driving CPT1a-mediated fatty acid oxidation. *Theranostics* **12**, 976–998. https://doi.org/10.7150/thno.63751 (2022).
19. Singer, M. et al. The third international consensus definitions for Sepsis and septic shock (Sepsis-3). *JAMA* **315**, 801–810. https://doi.org/10.1001/jama.2016.0287 (2016).
20. Fan, E., Brodie, D. & Slutsky, A. S. Acute respiratory distress syndrome: Advances in diagnosis and treatment. *JAMA* **319**, 698–710. https://doi.org/10.1001/jama.2017.21907 (2018).
21. Zhang, J. et al. YAP1 alleviates sepsis-induced acute lung injury via inhibiting ferritinophagy-mediated ferroptosis. *Front. Immunol.* **13**, 884362. https://doi.org/10.3389/fimmu.2022.884362 (2022).
22. Martinez-Ferriz, A., Ferrando, A., Fathinajafabadi, A. & Farras, R. Ubiquitin-mediated mechanisms of translational control. *Semin Cell. Dev. Biol.* **132**, 146–154. https://doi.org/10.1016/j.semcdb.2021.12.009 (2022).
23. Robinson, N. et al. Programmed necrotic cell death of macrophages: Focus on pyroptosis, necroptosis, and parthanatos. *Redox Biol.* **26**, 101239. https://doi.org/10.1016/j.redox.2019.101239 (2019).
24. van der Poll, T., van de Veerdonk, F. L., Scicluna, B. P. & Netea, M. G. The immunopathology of sepsis and potential therapeutic targets. *Nat. Rev. Immunol.* **17**, 407–420. https://doi.org/10.1038/nri.2017.36 (2017).
25. Liu, C. et al. Alpha-linolenic acid pretreatment alleviates NETs-induced alveolar macrophage pyroptosis by inhibiting pyrin inflammasome activation in a mouse model of sepsis-induced ALI/ARDS. *Front. Immunol.* **14**, 1146612. https://doi.org/10.3389/fimmu.2023.1146612 (2023).
26. Liu, B. et al. BRD3308 suppresses macrophage oxidative stress and pyroptosis via upregulating acetylation of H3K27 in sepsis-induced acute lung injury. *Burns Trauma.* **12**, e33. https://doi.org/10.1093/burnst/tkae033 (2024).
27. Zhao, C. et al. USP50 regulates NLRP3 inflammasome activation in duodenogastric reflux-induced gastric tumorigenesis. *Front. Immunol.* **15**, 1326137. https://doi.org/10.3389/fimmu.2024.1326137 (2024).
28. Zuo, Y. et al. Vitamin C promotes ACE2 degradation and protects against SARS-CoV-2 infection. *EMBO Rep.* **24**, e56374. https://doi.org/10.15252/embr.202256374 (2023).
29. Jiang, H. et al. Pristimerin suppresses AIM2 inflammasome by modulating AIM2-PYCARD/ASC stability via selective autophagy to alleviate tendinopathy. *Autophagy* **20**, 76–93. https://doi.org/10.1080/15548627.2023.2249392 (2024).
30. Cui, Y. et al. Neutrophil extracellular traps induce alveolar macrophage pyroptosis by regulating NLRP3 deubiquitination, aggravating the development of septic lung injury. *J. Inflamm. Res.* **16**, 861–877. https://doi.org/10.2147/JIR.S366436 (2023).
31. Lee, J. Y. et al. The deubiquitinating enzyme, ubiquitin-specific peptidase 50, regulates inflammasome activation by targeting the ASC adaptor protein. *FEBS Lett.* **591**, 479–490. https://doi.org/10.1002/1873-3468.12558 (2017).

32. Tracz, M. & Bialek, W. Beyond K48 and K63: Non-canonical protein ubiquitination. *Cell. Mol. Biol. Lett.* **26**, 1. https://doi.org/10.1186/s11658-020-00245-6 (2021).
33. Tang, J. et al. Sequential ubiquitination of NLRP3 by RNF125 and Cbl-b limits inflammasome activation and endotoxemia. *J. Exp. Med.* **217** https://doi.org/10.1084/jem.20182091 (2020).
34. Rahman, S. & Wolberger, C. Breaking the K48-chain: Linking ubiquitin beyond protein degradation. *Nat. Struct. Mol. Biol.* **31**, 216–218. https://doi.org/10.1038/s41594-024-01221-w (2024).
35. Lim, K. L. & Lim, G. G. K63-linked ubiquitination and neurodegeneration. *Neurobiol. Dis.* **43**, 9–16. https://doi.org/10.1016/j.nbd.2010.08.001 (2011).

Author contributions
All authors participated in the design, interpretation of the studies and analysis of the data and review of the manuscript. S H drafted the work and revised it critically for important intellectual content; J H, S S and Y C were responsible for the acquisition, analysis and interpretation of data for the work; L W made substantial contributions to the conception or design of the work. All authors read and approved the final manuscript.

Funding
The authors declare that no funds, grants, or other support were received during the preparation of this manuscript.

Declarations

Competing interests
The authors declare no competing interests.

Ethical approval and consent to participate
This study was approved by the Ethics Committee of Hangzhou TCM Hospital Affiliated to Zhejiang Chinese Medical University. Informed consent was obtained from all individual participants included in the study. This study was performed in line with the principles of the Declaration of Helsinki. All animal experiments should comply with the ARRIVE guidelines. All methods were carried out in accordance with relevant guidelines and regulations.

Additional information
Supplementary Information The online version contains supplementary material available at https://doi.org/10.1038/s41598-025-11224-2.

Correspondence and requests for materials should be addressed to L.W.